Escola de Primavera de Transição e Turbulência
Blumenau 2022

ABCM
13th Spring School on Transition and Turbulence
September 19th-23rd, 2022, Blumenau, SC, Brazil

EPTT-2022-0035
Hot-wire measurements on the Ahmed body turbulent wake in a low-speed wind tunnel

Marcelo I. Adotti
Instituto de Modelado e Innovación Tecnológica IMIT (Consejo Nacional de Investigaciones Científicas y Técnicas - Universidad Nacional del Nordeste. Argentina)
italoadotti@conicet.gov.ar
Adrián R. Wittwer
Laboratorio de Aerodinámica - Facultad de Ingeniería - Universidad Nacional del Nordeste. Argentina.
a_wittwer@yahoo.es
Juan M. Rodriguez
Instituto de Modelado e Innovación Tecnológica IMIT (Consejo Nacional de Investigaciones Científicas y Técnicas - Universidad Nacional del Nordeste. Argentina)
Jorge O. Marighetti
Laboratorio de Aerodinámica - Facultad de Ingeniería - Universidad Nacional del Nordeste. Argentina.
Beatriz A. Iturri
Instituto de Modelado e Innovación Tecnológica IMIT (Consejo Nacional de Investigaciones Científicas y Técnicas - Universidad Nacional del Nordeste. Argentina)
Hugo Castro
Instituto de Modelado e Innovación Tecnológica IMIT (Consejo Nacional de Investigaciones Científicas y Técnicas - Universidad Nacional del Nordeste. Argentina)
Mario E. De Bortoli
Laboratorio de Aerodinámica - Facultad de Ingeniería - Universidad Nacional del Nordeste. Argentina.
Gisela M. Alvarez y Alvarez
Laboratorio de Aerodinámica - Facultad de Ingeniería - Universidad Nacional del Nordeste. Argentina.

Abstract. *The Ahmed body is a standard model proposed for the study of road vehicles, serving as a reference point for calibrating wind tunnels, computer codes, and for extrapolating results for design or industrial purposes. Even though the model is a simple geometry, it reproduces the turbulent flow of the wake, boundary layer separations and flow re-entries, in a similar way to those found in real ground vehicles. Particularly, the study of turbulent wakes is of interest to evaluate possible effects of instability due to dynamic loads introduced by the wind, aiming to reduce fuel consumption. In this paper, measurements of the Ahmed body's wake are reported. The experiments have been carried out in the wind tunnel "Jacek Gorecki" of the Universidad Nacional del Nordeste (UNNE), Argentina. The measurements were performed with a DANTEC hot wire anemometer. A previous calibration of a single probe was carried out within the range of speed measurements, and then time velocity series were obtained at the wake turbulent flow. The preliminary mean velocity results are evaluated and compared with a Laser Doppler Anemometry (LDA) experiment from specific literature. Spectral analysis of the velocity fluctuations for relevant measurement points is also presented.*

Keywords: *Ahmed body, Turbulence, CTA, Wind Tunnel*

1. INTRODUCTION

The model proposed by Ahmed *et al.* (1984) is one of the most popular studied geometries in road vehicles aerodynamics. Numerous experimental and numerical test have been carried out through the last forty years with generic road vehicle models, Le Good and Garry (2004) shows that is a good strategy to determine fundamental aerodynamic characteristics. Over the years experimental works evaluated symmetrical and cross flow conditions, for different Reynolds numbers, measuring forces and flow characteristics for the Ahmed body. These experimental tests used different measurement techniques, some of them are: drag balance, pressure taps, hot-wire anemometer (CTA), laser doppler anemometer (LDA) or particle image velocimetry (PIV) (Lienhart *et al.*, 2002; Conan *et al.*, 2005; Meile *et al.*, 2016).

Numerical simulations provide more detailed information on wake turbulence flow variables, and many authors obtain good agreement with experimental tests. One of the most widely used numerical simulation techniques is the Reynolds-averaged Navier-Stokes Equations (RANS), which through turbulence models obtain good results evaluating global force coefficients, and vortical structures are well represented (Meile *et al.*, 2011; Adotti *et al.*, 2017). In counterpart, these models, losses the capability to predict correctly the partial detachment of the mean flow over the slant tail producing some discrepancies in the lift coefficient.

Large eddy simulation (LES) technique (Krajnović and Davidson, 2004; Minguez *et al.*, 2008; Franck *et al.*, 2009;

Castro *et al.*, 2010) do not show problems to predict correctly flow reattachment and global force coefficients, but is most computationally expensive especially at high Reynolds numbers.

Our work presents a test to characterise and contrast symmetric mean velocity profiles with previous cited works and evaluate the signature of spectrum of velocity fluctuations with its corresponding correlation functions. The paper is organised as follows: section 2 presents the Ahmed body and its principal wake flow characteristics, section 3 describes the instrumentation and experimental used technique, section 4 presents and analyses the results, and, finally, section 5 discusses conclusions and further works.

2. MODEL AND WAKE FLOW CHARACTERISTICS

The Ahmed body's geometric configuration used in the test corresponds to a tail angle of $\beta = 35°$, and a 1:1 scale, Fig. 1. The evaluated shape is critical because it produces an early detachment of the boundary layer and subsequent flow separation over the body, generating a more complex wake turbulence than other tilted tail configurations (Ahmed *et al.*, 1984; Meile *et al.*, 2016).

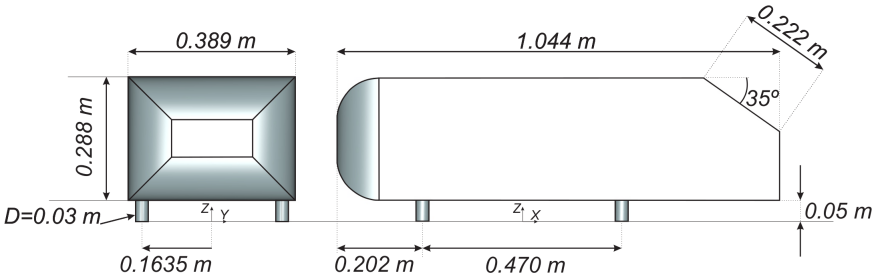

Figure 1. Ahmed body - slant β =35º (Adotti *et al.*, 2017).

The main features in the wake flow of Ahmed's body are related to; its tail angle configuration, Reynolds number and ground clearance, Fig. 2. Aerodynamic forces generated by the wake depends on body geometric configuration and incident flow, these represent a large part of the total forces acting on the body. Under certain conditions, the wake can become unstable, cases have been reported for Re 10^5 (Grandemange *et al.*, 2013) and long time scales where the wake becomes bi-stable, breaking flow symmetry downstream body. As a consequence, the forces acting on the body are transient (Meile *et al.*, 2016). In our work, measured series are not long enough to detect symmetry breaking of the flow in the wake, compared to the time series of the works cited above.

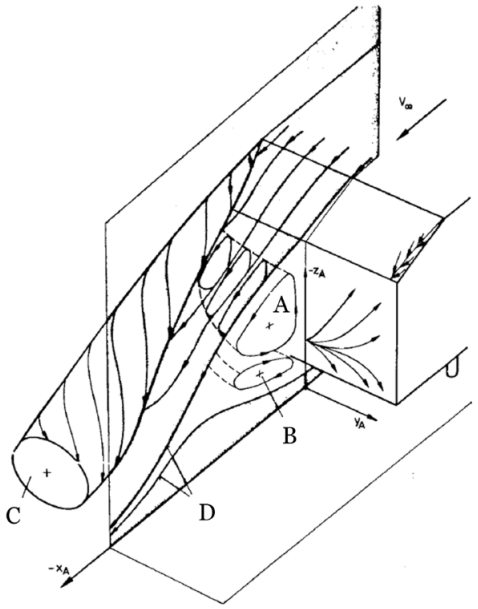

Figure 2. Generic vortex system in wake (Ahmed *et al.*, 1984).

Assuming wake flow symmetry, vortexes "A", "B" and "C" are correlated, and the intensity of "A" and "C" feed each other. If the flux on the inclined surface remains attached, the force of "C" depends on the angle β and, therefore, the force of "A". Vortex "B" intensity depends on the Reynolds number and the distance to the ground. The vortices "A" and "B" are enclosed in a separation bubble "D". All these vortices and the angle β are indirectly related (Ahmed *et al.*, 1984).

These are the most studied features in the turbulent wake of Ahmed's body, and will be use later to discuss results in combination with flow statistics and spectral analysis.

3. INSTRUMENTATION AND EXPERIMENTAL TECHNIQUE

The experiments were carried out in the "Jacek P. Gorecki" wind tunnel at UNNE, Argentina (Wittwer and Möller, 2000). Figure 3 shows the configuration and position of Ahmed's body in the test section number 1 of wind tunnel. The model is mounted a few meters from the convergent inlet zone, since a thick boundary layer is not necessary. This configuration guarantees incident flow turbulence intensities of less than 1% in agreement with Lienhart *et al.* (2002) and Meile *et al.* (2016).

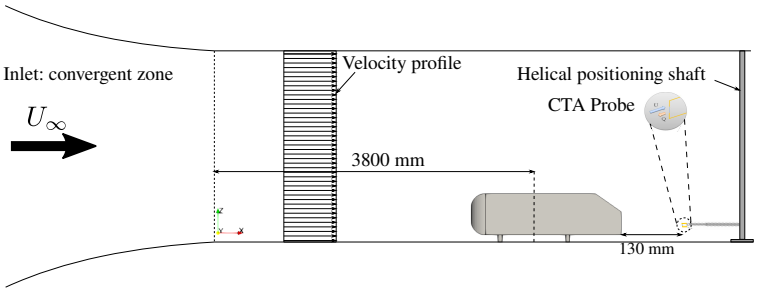

Figure 3. Layout of CTA and the Ahmed body.

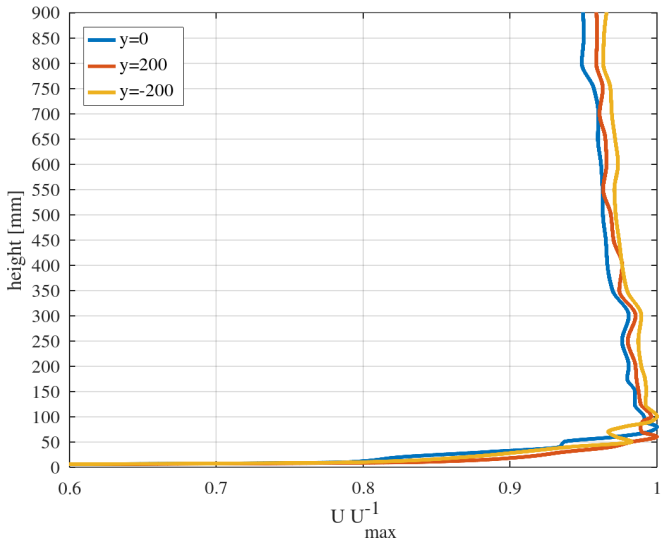

Figure 4. Dimensionless velocity profiles of incident flow.

The incident wind corresponds to a uniform turbulent flow, with a turbulence intensity outside the boundary layer of less than 0.7%. Dimensionless mean inlet velocities profiles relative to their maximum values (y=0 mm, y=-200 mm and y=200 mm) are shown in Fig. 4, indicating a variability of the order of 5% outside the boundary layer. These three positions covers the front section of Ahmed's body. The measurements in the wake were made with a DANTEC "single-wire" hot-wire anemometer, the signal was amplified and filtered previously to the input data acquisition system (analog/digital converter). Post-processing was performed with the free software GNU Octave, a simplified scheme shows in, Fig. 5, the acquisition steps.

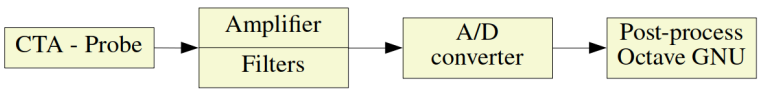

Figure 5. Acquisition system block diagram.

Velocity measurements in the wake of Ahmed's body were made with the probe located in y=0 mm, and at a distance x=130 mm downstream of the model, measuring twelve different "z" heights distributed between z=15 mm and z=410 mm. Representative numerical series of velocity were obtained by a sampling frequency of 2048 Hz during 128 seconds.

An electronic low-pass filter set at 1000 Hz was connected prior to A/D signal conversion. The CTA probe was calibrated carrying out within the range of velocity measurements employing a 4th degree polynomial function.

The Reynolds number (Re) is defined by the mean reference velocity U_∞ and the length $L = 1.044$ m of the Ahmed body, being ν the kinematic viscosity of air, Eq. 1, and the test value of Re is 1.66×10^6. Some authors calculate the Reynolds number with the height $H = 0.288$ m, changing the test value to Re = 4.512×10^5.

$$Re = \frac{U_\infty L}{\nu} \tag{1}$$

4. RESULTS

After a comparative analysis between the velocities obtained in this test and those published by Lienhart *et al.* (2002), it is possible to assume that when placing the CTA probe in the vertical plane "x-z" it measures only longitudinal velocities due to wake symmetry. Lateral velocities can be neglected, because their contribution to the module of the velocity vector evaluated in the plane is less than 1%. This allows us to assume that the velocity vector in the plane "x-z" is equal to the longitudinal velocity vector defined by Eq. 2 defined as the sum of the mean $\langle U \rangle$ and the fluctuating u component of the velocity spectrum.

$$\{|U^2 + V^2|\} = \{U\} = \langle U \rangle + u \tag{2}$$

Table 1. Main characteristic parameters at the wake (y=0 mm, x=130 mm).

Height "z" [mm]	$\langle U \rangle$ [m/s]	σ_u [m/s]	L_{uu} [m]
15	23.305	3.926	0.071
30	20.205	5.296	0.060
50	10.125	4.523	0.031
90	8.256	2.731	0.023
130	6.828	2.429	0.033
170	4.316	1.963	0.030
210	3.162	1.440	0.013
250	7.526	2.950	0.038
290	20.870	2.865	0.074
330	23.962	0.503	0.046
370	23.517	0.238	1.703
410	23.347	0.160	2.513

In this section the results obtained in the tests described in the previous section are presented. The main characteristics of the measuring points; height z, mean velocity $\langle U \rangle$, standard deviation σ_u and integral length scale L_{uu} are indicated in Tab. 1.

The mean velocity profile and the spectra with their auto-correlation functions corresponding to the fluctuating longitudinal velocities, obtain in twelve measurements points, are shown, Fig. 3. Finally, the calculated values of integral length scale for measured points are discussed.

4.1 Dimensionless Mean Velocity Profile

The dimensionless mean velocity was defined by Eq. 3, were $\langle U \rangle$ is the mean velocity for a analysed "z" point and $\langle U_\infty \rangle$ is the mean reference velocity.

$$U^* = \left\langle \frac{U}{U_\infty} \right\rangle \tag{3}$$

Figure 6 shows the results (dashed blue line) contrasted with an experimental test performed with a LDA by Lienhart *et al.* (2002) (solid light blue line). The CTA probe used cannot differentiate the incident flow angle and cannot detect negative values. Therefore, to estimate the characteristic re-circulation zone in the wake (Ahmed *et al.*, 1984), the negative pressure values obtained by a Pitot probe mounted with the CTA are used. In this way, the sign of mean velocity values located in the area in question is changed (z=90 mm to z=210 mm) (solid red line).

The profile location x=187 mm of Lienhart *et al.* (2002) was selected instead others evaluated profiles after a similitude analysis. Firstly, exists some differences; the Reynolds number for this test is 40% lower than the previous cited work, and secondly, the positioning system used in this test can provide some alignment errors transmitting them to the CTA probe. This differences allows selecting the mentioned profile to compare similar wake flow characteristics. In general, a good fit is observed in the lowest zones of the profile from z= 15 mm to z= 90 mm and for the point z=210 mm, the remaining points of the profile present differences of the order of the standard deviation.

Furthermore, turbulence intensity is also presented as the dimensionless standard deviation σ/U_∞, in Fig. 6. Intensity values at points z=15 mm to z=50 mm are the highest, influenced by the flow that slips under the body. The re-circulation zone, z=90 mm to z= 210 mm, has intensity values 75% lower than the previous points. An increase in intensity is shown for the points z=250 mm and z=290 mm, influenced by possible effects of the flow that breaks off from the tail of the body and the top of the re-circulation bubble "C". The remaining points, z=330 mm to z=410 mm, have turbulence intensities similar to the incident free flow.

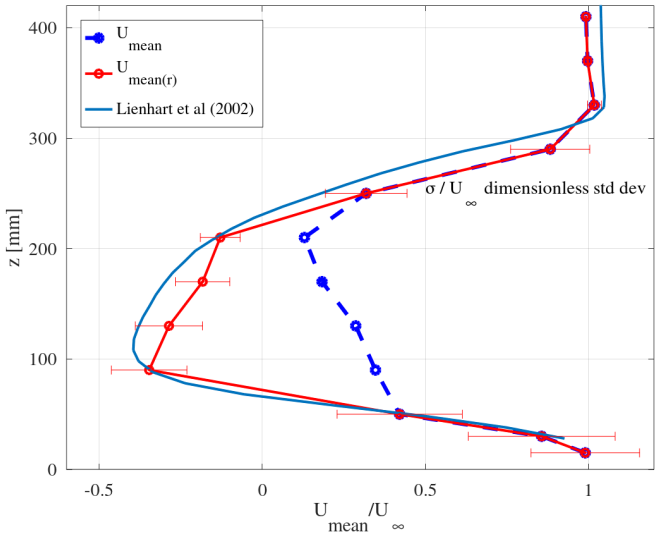

Figure 6. Dimensionless mean velocity profile. Horizontal solid red line represents dimensionless standard deviation.

4.2 Spectral Analysis of Velocity Fluctuations

The auto-spectral density function or power spectrum represents the variation in function of frequency of the mean square value of the velocity fluctuation as a function of time $u(t)$ provided by a continuous number series acquired with a time interval t, and it is expressed by Eq. 4:

$$S_u(f) = \frac{1}{B_e T} \int_0^T u^2(f, B_e, t) dt \tag{4}$$

B_e is the bandwidth (spectrum resolution), and T is a suitable integration time depending on the scales of turbulence. The spectra resolution depend on the number of blocks and number of values per block, the used configuration is 96 blocks of 2048 values. The Danielson-Lanczos Lemma is used to solve the discrete form of Eq. 4 (Wolberg, 1988), using a script based on Press *et al.* (2007) and Johnson (1988).

Figure 7, Fig. 8 and Fig. 9 shows the obtained spectra. They are organised into three groups depending on height z, where their value in millimetres accompanies the variable as a label, group 1 (z15, z30, z50), group 2 (z90, z130, z170, z210, z250), and group 3 (z290, z330, z370, z410). The left plots represent the power spectrum density function-frequency in SI units. The right plots shows the dimensionless spectrum in the ordinate axis, but the wavelength with dimension $[L^{-1}]$ is indicated in the abscissa axis.

Figure 7 shows the spectra group 1, these measurements are located downwind Ahmed's body in close proximity to the ground. Fig. 6 shows the mean velocity magnitude decrease with height. Although, in Fig. 7, for z=15 mm the lowest turbulence kinetic energy is obtained in coincidence with the lowest bound of the separation bubble "D" in Fig. 2. Is not clearly detected a singular frequency on these spectra. The plot on the left shows from 1 to 20 Hz a zone with major energy; then as the frequency increases energy decays and follows Kolmogorov's -5/3 power law slope. The semi-dimensionless graph on the right shows, for large-scale eddies, in a range of 1 and 4 m^{-1}, a not well defined wave number, especially for z15 and z30 where this behaviour is more evident.

Figure 8 shows spectra group 2, inside the separation bubble “D”. The reverse flux is well captured in this zone and is represented in the dimensionless mean velocity profile with negative values, Fig. 6. The evaluated points have the same behaviour, characterised for a similar energy content within the range analysed, particularly the z210 point show low energy than others, which is expected because it is the lowest velocity fluctuation of the group, presented in Tab. 1 like standard deviation σ_u. The left plot shows the begin of the energy decay for the spectra near 20 Hz, coincident with the -5/3 power law Kolmogorov. In the dimensionless right plot it is not possibly distinguish any indication of a particular characteristic value of wave number, only slightly observable at very blurring range within 1 to 200 m^{-1}.

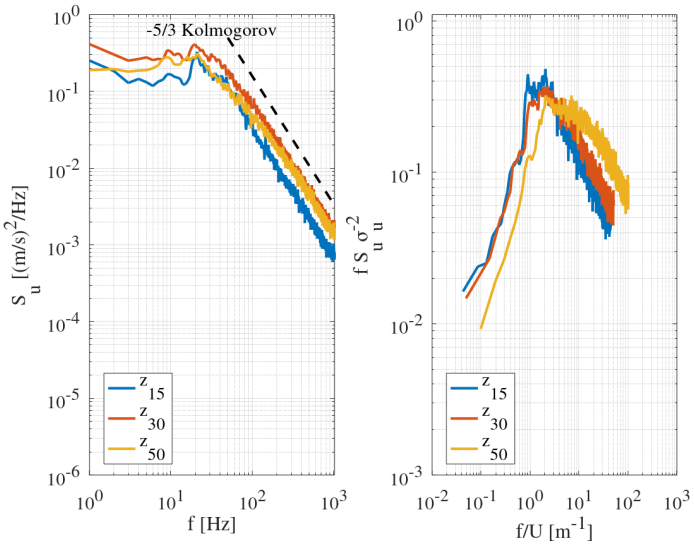

Figure 7. Spectra group 1.

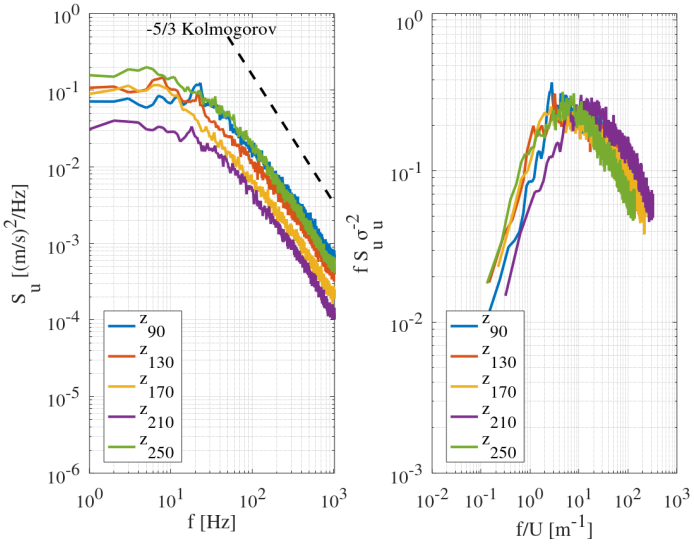

Figure 8. Spectra group 2.

Figure 9 shows the spectra group 3, their behaviour is clearly different from that of the previous groups. The evaluated points are located in the upper zone of the Ahmed body. Analysing the left plot it is possible consider the z410 point like a free flow spectrum, being positioned 72 mm above Ahmed’s body. The z290 point seems still on the near upper bound of the separation bubble “D”, because preserve the characteristic slope of energy decay similar to group 2, which is not present in the others evaluated points. However, it begins to show a spectral peak that is later clearly manifested in z330 and z370 within range 50 to 70 Hz. In addition z330 has a singularity peak near 150 Hz. The right plot allows distinguish the same behaviour than left plot, is evident a marked peak of energy for z330 and z370 points. The z290 point shows a little less energy in the same maximum range of z370. The peaks are displayed for a wave number within range 2 a 6 m^{-1}. The z330 point shows a singularity peak in 6 m^{-1} wave number.

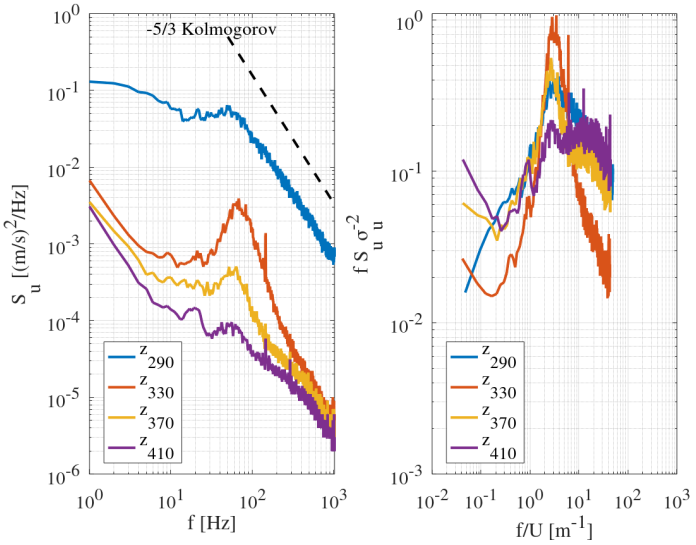

Figure 9. Spectra group 3.

4.3 Correlation function of velocity fluctuations

Assuming a statistically steady flow, the origin of time could be considered irrelevant, so the correlation between $u(t)$ and $u(t')$ depend only on time difference $t' - t = \tau$ (Tennekes and Lumley, 1978). Consequently, a correlation function $R_{uu}(\tau)$, Eq. 5, and coefficient $C_{uu}(\tau)$ are defined Eq. 7.

$$R_{uu}(\tau) = \langle u(t)u(t+\tau)\rangle \tag{5}$$

where $u(t)$ is the fluctuating component of velocity spectrum measured, and $u(t+\tau)$ a instant τ later.

$$R_{uu}(0) = \langle u(t)u(t+0)\rangle = \left\langle u(t)^2\right\rangle \tag{6}$$

When $\tau = 0$ the correlation function is equal to variance of velocity fluctuations, normally is used to normalise the auto-correlation function expressed for the coefficient $C_{uu}(\tau)$.

$$C_{uu}(\tau) = \frac{R_{uu}(\tau)}{R_{uu}(0)} \tag{7}$$

All correlation coefficients are evaluated in a time windows of 4.88 seconds. A window is inserted in the figures Fig. 10, Fig. 11 and Fig. 12 to better visualise the behaviour of the functions at low τ.

Figure 10 shows the correlation coefficients of the group, a strong gradient and an early crossing over the x-axis are evident. The behaviour of z15, z30 and z50 are similar and shows a rapid non-correlation of velocity fluctuations. In the first 0.2 seconds it is possible to distinguish a sinusoidal behaviour, then its amplitude decreases.

Figure 11 shows the correlation coefficients of group 2, equal to the previous group analysed, it has a strong slope at the initial time. All group points had a similar behaviour. There is no obvious correlation, only a sinusoidal behaviour characterised by a low amplitude value of the correlation coefficient is visible in the first 0.2 seconds, which then fades away.

Figure 12 shows correlation coefficients of group 3, clearly different from the previous groups, the point z290 has a fast gradient and about 0.1 seconds loses all correlation. The rest of the evaluated points shows a smooth gradient with a behaviour similar to a very low amplitude sinusoidal function.

4.4 Integral length scale

The integral length scale is introduced to analyse if there are large eddies or small vortices at different points. This length scale is calculated using Taylor's frozen turbulence hypothesis (Blessmann, 2013), evaluating the time scale τ_{uu}, defined by Eq. 8, and numerically integrating the discrete correlation coefficients defined in Eq. 7. The expression that relates the spatial and temporal scale, is defined by Eq. 9:

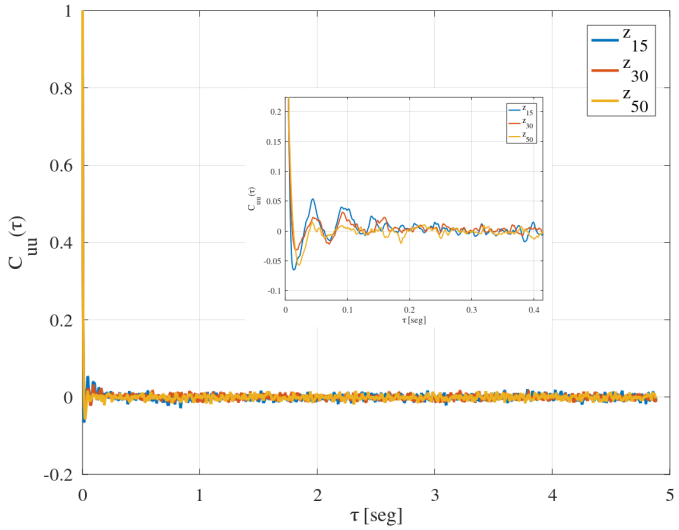

Figure 10. Correlation coefficients group 1.

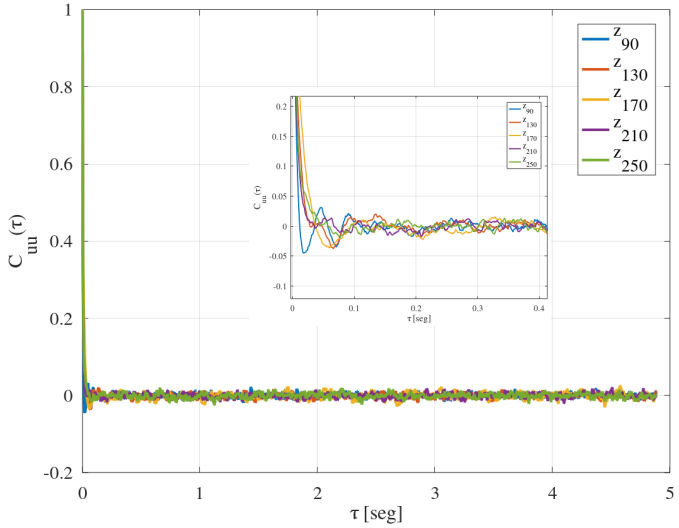

Figure 11. Correlation coefficients group 2.

$$\tau_{uu} = \int_0^\infty C_{uu}(z,\tau)d\tau \tag{8}$$

$$L_{uu} = \langle U \rangle \tau_{uu} \tag{9}$$

L_{uu} results are presented in Tab. 1, defining the same analysis group. Group 1: z15 to z50. Group 2: z90 to z250 and Group 3: z290 to z410.

Group 1 and group 2 show values of L_{uu} indicating small vortices existence, while group 3, mainly points z370 and z410, show values of L_{uu} suggesting large eddies associated with the main flow.

4.5 Discussion on spectral analysis and auto-correlation function

It is not possible to make a direct comparison of the spectral results and the auto-correlation functions obtained in this work with the values obtained by other authors. Based on the literature review carried out to date, it has been established that very few authors have undertaken studies of this type with similar parameters and objectives. Most of the experimental studies on Ahmed's body focus on the measurement of fluctuating pressures and not fluctuating velocities.

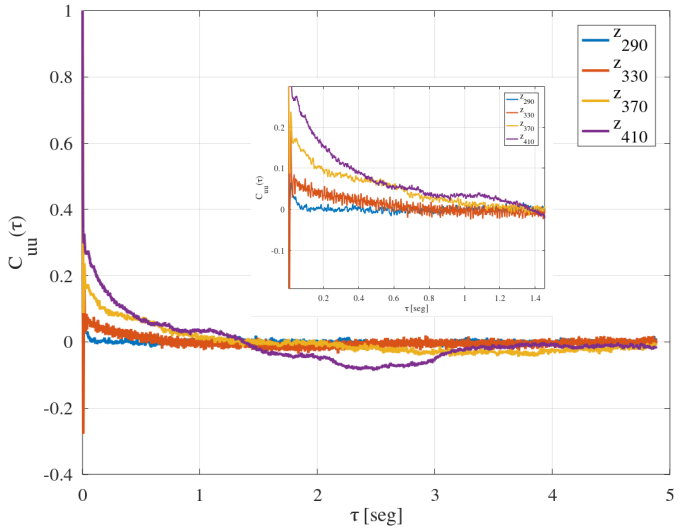

Figure 12. Correlation coefficients group 3.

Lienhart and Pêgo (2012) have performed a complementary work based on the tests carried out in the article by Lienhart *et al.* (2002) for the 25º slant tail angle configuration. They have replicated the flow conditions and measurement technique. Compared to our work, and even though the geometric and Re differences, spectral power density functions have a similar behaviour, in particular for the upper low-frequency spectral peaks. Also analogous characteristic times of the temporary auto-correlation functions for homologous analysis points located in the wake are observed. It is important to note that Lienhart and Pêgo (2012) have carried out measurements for 330 seconds with an acquisition frequency of 1500 Hz, being able thus to visualise the bi-stable behaviour of the velocity time series for an analysis point located in the lower zone of the wake, particularly between the flow that drains under the body and the re circulation zone "B". It should be remembered that in our work it has not been possible to detect this instability.

The experimental study by Tunay *et al.* (2014) was developed in an H2O channel with Re number values much lower than those used in this work. However, what practically prevents a comparison of the spectral results shown in that article with those obtained in our analysis is the type of instruments for measuring fluctuating velocities and the objectives that are set in each case. In Tunay *et al.* (2014) article, the measurements were made with PIV (Particle Image Velocimetry) with much lower acquisition frequencies and the analysis points were restricted to specific areas of behaviour that indicate vortex shedding. Thus, the spectra shown there are limited to the range between 0 and 7 Hz.

Murzyn *et al.* (2017) made an interesting report from LDA (Laser Doppler Anemometry) measurements on the wake of Ahmed's body using a wind tunnel. Although the range of frequencies analysed and the characteristic parameters of the tests differ considerably from our study, the characteristic frequencies of the upper spectral peak indicate values similar to those obtained at almost homologous points. However, it is important to mention that the comparison that we can make is very partial since the objective of the report is the analysis of the variation of the Strouhal number in specific areas of the wake.

5. CONCLUSIONS

In this work, the mean velocities measured in the turbulent wake of the Ahmed body with hot-wire anemometer are analysed and compared with LDA tests performed in a previous work. The fluctuating velocity standard deviation is also presented to characterise the turbulent flow. In addition, a spectral power function analysis of fluctuating velocities is performed, grouping them according to its different wakes zones. From this analysis it is possible to infer the characteristics associated with the well-known symmetrical configuration in the wake of the Ahmed body, due to the different turbulent energy according to the "z" position. It is possible to determine the small vortex area affected by the Ahmed body and the large eddy area associated with the main flow. In future works, the symmetry breaking of the wake will be evaluated with longer time series using the same measurement technique. Non-stationary bi-stable behaviour observed in other works, may be analysed from these next experimental studies.

6. REFERENCES

Adotti, M.I., Castro, H.G., Paz, R.R. and De Bortoli, M., 2017. "Simulación computacional del cuerpo de Ahmed bajo Distintos ángulos de incidencia de viento". *Asociación Argentina de Mecánica Computacional. AMCA*, Vol. 37. ISSN

2591-3522.

Ahmed, S.R., Ramm, G. and Faitin, G., 1984. "Some salient features of the time - averaged ground vehicle wake". *SAE Transactions*, pp. 473–503.

Blessmann, J., 2013. *O vento na engenharia estrutural*. Editora da UFRGS, 2nd edition. ISBN 9788538602040.

Castro, G., Paz, R., Storti, M., Sonzogni, V., Marighetti, J. and Bortoli, M., 2010. "Experimental and numerical study of the aerodynamic behaviour of a simplified road vehicle". *Asociación Argentina de Mecánica Computacional. AMCA*, Vol. 32. ISSN 2591-3522.

Conan, B., Anthoine, J. and Planquart, P., 2005. "Experimental aerodynamic study of a car-type bluff body". *Experiments in Fluids*, Vol. 50, pp. 1273–1284. doi:10.1007/s00348-010-0992-z.

Franck, G., Nigro, N., Storti, M. and D´ Elía, J., 2009. "Numerical simulation of the flow around the Ahmed vehicle model". *Latin American applied research. Pesquisa aplicada latino americana. Investigación aplicada latinoamericana.*, Vol. 39, pp. 295–306.

Grandemange, M., Gohlke, M. and Cadot, O., 2013. "Turbulent wake past a three-dimensional blunt body. part 1. global modes and bi-stability". *Journal of Fluid Mechanics*, Vol. 722, p. 51–84. doi:10.1017/jfm.2013.83.

Johnson, D.K., 1988. "A data analysis system for unsteady turbulence measurements". *Monterrey, California. Naval Postgraduate School*.

Krajnović, S. and Davidson, L., 2004. "Large-eddy simulation of the flow around simplified car model". *In 2004 SAE World Congress. Detroit, Michigan, USA.*, Vol. SAE Paper 2004-01-0227.

Le Good, G. and Garry, K., 2004. "On the use of reference models in automotive aerodynamics". *SAE Technical Paper 2004-01-1308*. doi:10.4271/2004-01-1308.

Lienhart, H. and Pêgo, J., 2012. "Spectral density and time scales of velocity fluctuations in the wake of a simplified car model". *SAE Technical Papers*. doi:10.4271/2012-01-0592.

Lienhart, H., Stoots, C. and Becker, S., 2002. "Flow and turbulence structures in the wake of a simplified car model (ahmed model)". *Notes on Numerical Fluid Mechanics*, Vol. 77.

Meile, W., Brenn, G., Reppenhagen, A., Lechner, B. and Fuchs, A., 2011. "Experiments and numerical simulations on the aerodynamics of the Ahmed body". *CFD Letters*, Vol. 3.

Meile, W., Ladinek, T., Brenn, G., Reppenhagen, A. and Fuchs, A., 2016. "Non-symmetric bi-stable flow around the Ahmed body". *International Journal of Heat and Fluid Flow*, Vol. 57, pp. 34–47.

Minguez, M., Pasquetti, R. and Serre, E., 2008. "High-order large-eddy simulation of flow over the "Ahmed body" car model". *Physics of Fluids - PHYS FLUIDS*, Vol. 20. doi:10.1063/1.2952595.

Murzyn, F., Bouillaut, V., Mehel, A. and Felder, S., 2017. "Non-stationary flow downstream of an Ahmed body: frequency analysis and preliminary assessment of the triple decomposition technique". Technical report, Water Research Laboratory, University of New South Wales. School of Civil and Environmental Engineering.

Press, W., Teukolsky, S., Vetterling, W. and Flannery, B., 2007. *Numerical Recipes: The Art of Scientific Computing*. Cambridge University Press, 3rd edition. ISBN 9780521880688.

Tennekes, H. and Lumley, J., 1978. *A FIRST COURSE IN TURBULENCE*. MIT PRESS.

Tunay, T., Sahin, B. and Ozbolat, V., 2014. "Effects of rear slant angles on the flow characteristics of Ahmed body". *Experimental Thermal and Fluid Science*, Vol. 57, pp. 165–176. ISSN 0894-1777.

Wittwer, A. and Möller, S., 2000. "Characteristics of the low-speed wind tunnel of the UNNE". *Journal of Wind Engineering and Industrial Aerodynamics - J WIND ENG IND AERODYN*, Vol. 84, pp. 307–320. doi:10.1016/S0167-6105(99)00110-5.

Wolberg, G., 1988. "Fast fourier transforms: A review". *Columbia Academic Commons*.

7. RESPONSIBILITY NOTICE

The authors are the only responsible for the printed material included in this paper.